UCRL-TR-220712

LAWRENCE
LIVERMORE
NATIONAL
LABORATORY

LCLS XTOD Attenuator System System Concept Report

K. Kishiyama, M. Roeben, J. Trent, D. Ryutov, S. Shen

April 19, 2006

Disclaimer

This work was performed under the auspices of the U.S. Department of Energy by University of California, Lawrence Livermore National Laboratory under Contract W-7405-Eng-48.

LCLS XTOD Attenuator System

System Concept Report

New Technologies Engineering Division
Lawrence Livermore National Laboratory

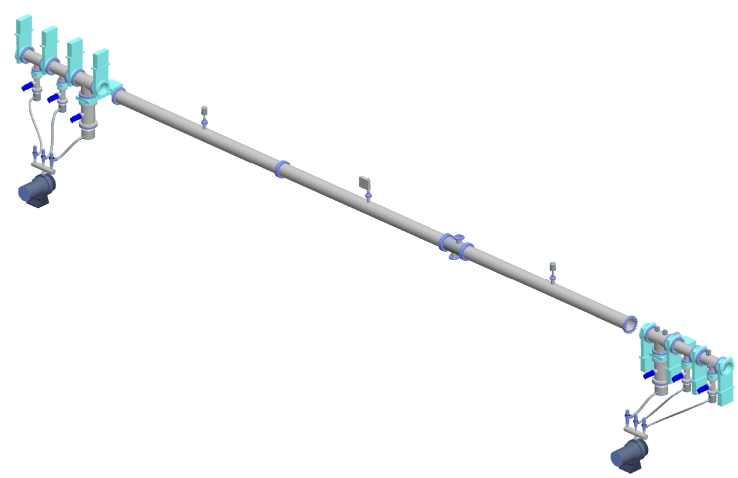

Submitted to: LCLS SLAC
April 14, 2006

Disclaimer

This work was performed under the auspices of the U.S. Department of Energy by University of California, Lawrence Livermore National Laboratory under Contract W-7405-Eng-48.
Work supported in part by the DOE Contract DE-AC02-76SF00515. This work was performed in support of the LCLS project at SLAC.

TABLE OF CONTENTS

1 Introduction

The attenuator system for the Linac Coherent Light Source (LCLS) X-ray Transport, Optics and Diagnostics (XTOD) system has been configured and analyzed by the Lawrence Livermore National Laboratory's New Technologies Engineering Division (NTED) as requested by the SLAC/LCLS program. The system layout, performance analyses and selection of the vacuum components are presented in this System Conceptual Review (SCR) report. Also included are the plans for prototype, procurement, mechanical integration, and the cost estimates.

1.1 Physics Requirements

Requirements listed in LCLS-PRD-1.5-003 "Physics Requirements for the XTOD Attenuator System" [1] are summarized in Table 1.1.1.

Category	Subject	Requirement
General	**Energy Range**	FEL photon energy from 826.5 eV to 8265 eV.
	Attenuation Range	Up to 4 orders of magnitude
	Accuracy & Repeatability	Stable, reproducible attenuation for repeated FEL shots. Within 1.5% for attenuation factor of 10. Within 5% for attenuation factor of 10,000. Uniformity of attenuation over transverse dimension of the FEL beam is better than 1 % for all attenuation levels.
	Mechanical-Vacuum Design	Consistent with PRD 1.5-002, "XTOD Mechanical-Vacuum Systems."
	Discrete levels for solid attenuation	At least 3 steps for every decade of attenuation, up to 10^4.
	Space	Consistent with FEE environment for installation, operation and maintenance
Optics	**Aperture –"in-operation"**	permit un-obstructed passage of the full transverse extent (4σ) of the FEL photon beam
	Aperture – "fully open"	permit un-obstructed passage of the full transverse extent of the projected radiation field from the undulator, limited only by components upstream of the Front End Enclosure.
	Material Selection	limit the effect of scattered radiation and degradation of FEL beam transverse coherence, consistent with requirements of anticipated LCLS experiments.
Control	**System**	Fully-remote-controlled safe operation
	Level change time-Solid	Some seconds
	Level change time-gas	Several minutes.

Table 1.1.1: Physics Requirements

1.2 System Configuration

The attenuator system including both gas and solid scheme is to fit into a 10 m length of the Front End Enclosure (FEE) as illustrated in Fig. 1.2.1 and 1.2.2.

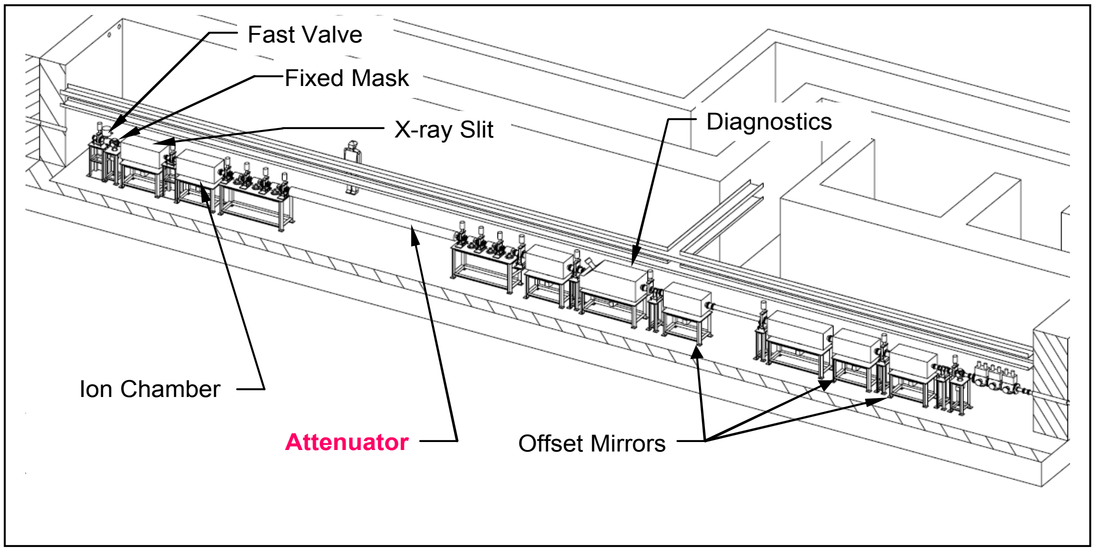

Fig. 1.2.1: Preliminary LCLS XTOD Front End Configuration

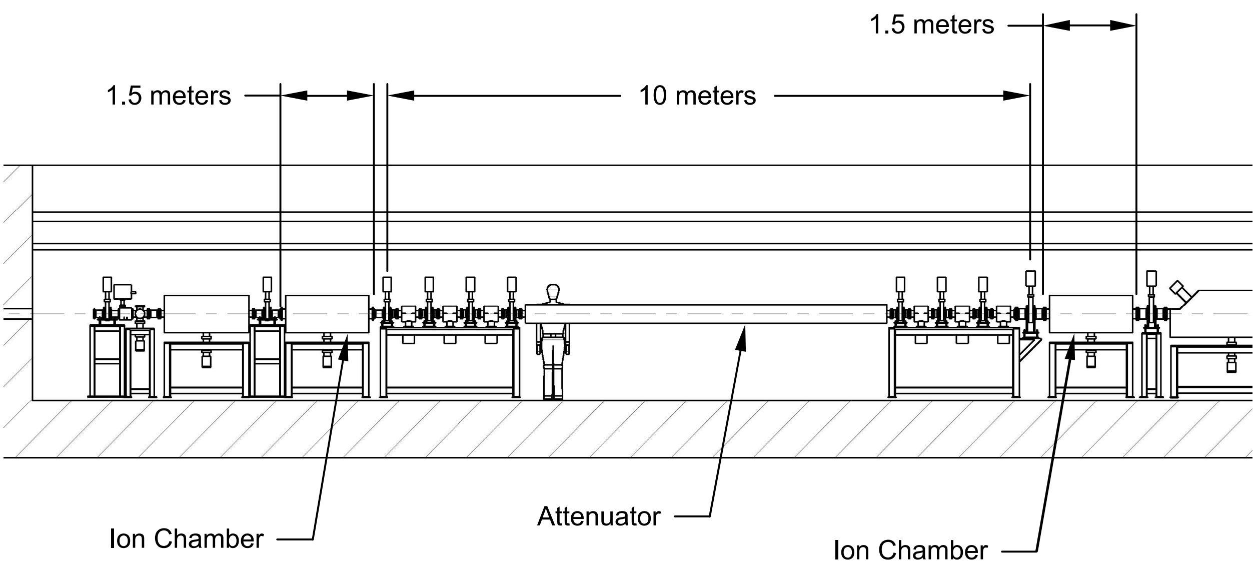

Fig. 1.2.2: Preliminary LCLS XTOD Attenuator Configuration

1.3 Deliverables

The System Concept Design effort includes designing a vacuum system that meets the pumping requirements and integrates with XTOD FEE structure. The report should address the following:

1. Design Objective
2. Physics Requirements
3. Technical/Performance Requirements
4. Organizational Interfaces
5. Technical Interface
6. ES&H and Assessment of Risk Areas
7. Prototype
8. Proposed Design Approach
    - System Design
    - Mechanical
    - Electrical
    - Software
9. Operations
10. Planned Test Program

The output of the SCR is a baseline design subject to the closure of any action items resulting from the review.

2 Design Approach

2.1 Aperture, Beam Clearance, and Alignment

The gas attenuator will be differentially pumped through a series of 3 mm diameter apertures drilled through 1 mm thick Be disks. The 3 mm diameter apertures allow the low energy FEL, which would be totally absorbed in the 1 mm thick Be, to freely pass through the system. The beryllium disks are also transparent to the spontaneous radiation, allowing the aperture to be aligned using the WFOVDI camera downstream. The beryllium windows will be mounted onto gate valves that separate the transition sections on either end of the main chamber. The gate valves can remove the windows when gas attenuator is not in use or when some of the other windows are being aligned. The transition sections each consist of 3 chambers separated from each other and the outside by 4 of the valve mounted windows. The 3 transition chambers on either end and their valves form a single rigid mechanical assembly isolated by bellows and with its own 4 degree-of-freedom (x,y, q,f) motorized alignment movers as shown in the **Fig. 2.1.1**.

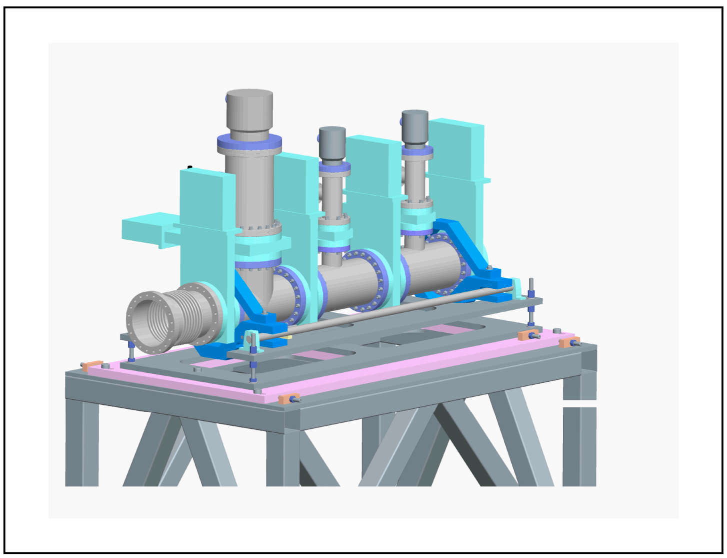

Fig. 2.1.1: Gate Valve with Beryllium Window

The 3 mm apertures in each section will be mechanically aligned during assembly to be collinear. The final alignment of each section to the low-energy FEL will be done by imaging the windows and the FEL with the wide-field-of-view direct imager located downstream.

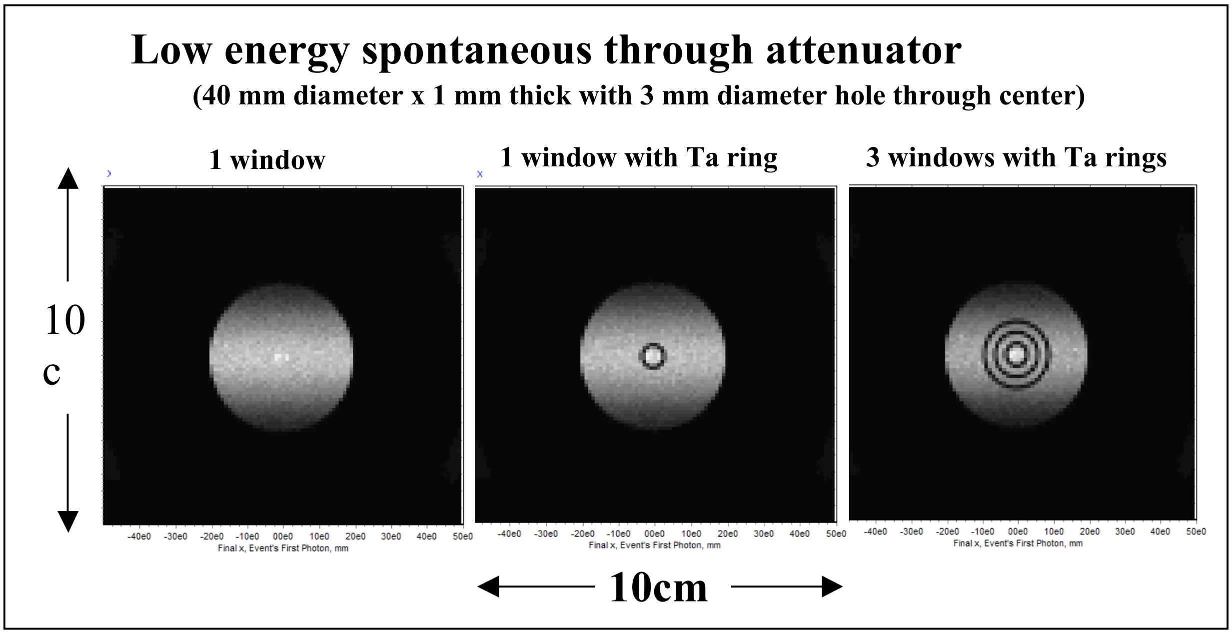

Fig. 2.1.2: Response of Low Energy Spontaneous Radiation Through Attenuator

Fig. 2.1.2 shows the response of the direct imager scintillator to the low energy spontaneous radiation from all 33 undulator segments. The image on the left is for one 1 mm thick Be window, assuming the other 9 or 13 are in the open position and out of the beam to avoid confusion. There is not much contrast in the image of the Be window even with this low energy radiation especially with the limited statistics of the simulation. The 3 mm diameter opening in the center is difficult to see but will be somewhat more obvious with the large number of photons in the real beam. Adding a ring of heavy material makes the center much easier to locate. The center image shows the result of bonding a 1 mm thick Ta ring to the back of the Be window, centered on the 3 mm diameter aperture. The position of the aperture is easily deduced from the position of the shadow of the Ta ring. The image on the right is through the 3 windows of the upstream section of the gas attenuator. Each window has a Ta ring of different diameter to aid identification.

Fig. 2.1.3 shows the response of the direct imager scintillator to the low energy spontaneous radiation accompanied by a saturated 826 eV FEL. The figure on the left, showing the image with all valves open, is dominated by the FEL. The middle figure has the 3 valves closed but the whole section is miss-aligned by 4.6 mRad and offset by 6 mm. Since the FEL cannot penetrate 1 mm of Be it is not visible. Nevertheless the Ta rings are visible in the spontaneous radiation that does make it through. We can tell that the large ring from the upstream end is in the correct position but the small ring in the downstream end is too high and make the necessary corrections to the position of the section. The figure on the right shows the resulting image after correcting the position of the section up to a residual 0.46 mRad tilt and 300 mm offset. The FEL is once again visible in the image. With this method it will be possible to locate the FEL and systematically align the apertures with the FEL *wherever it is located.*

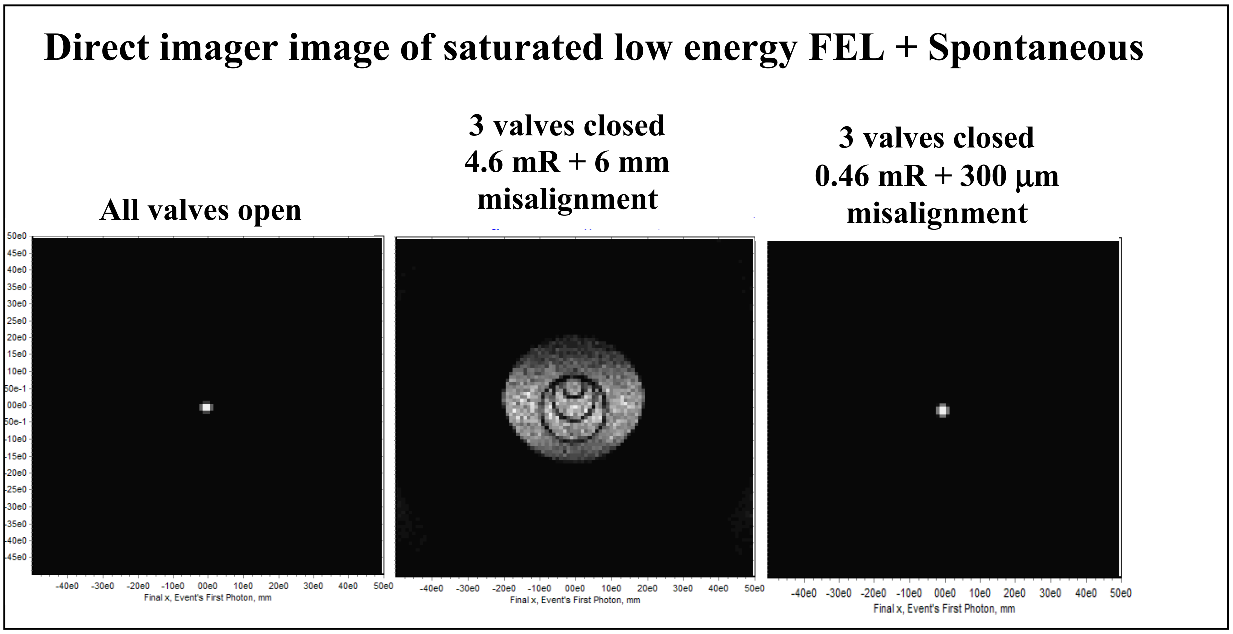

Fig. 2.1.3: Image of Saturated Low Energy FEL + Spontaneous

2.2 Solid Attenuation

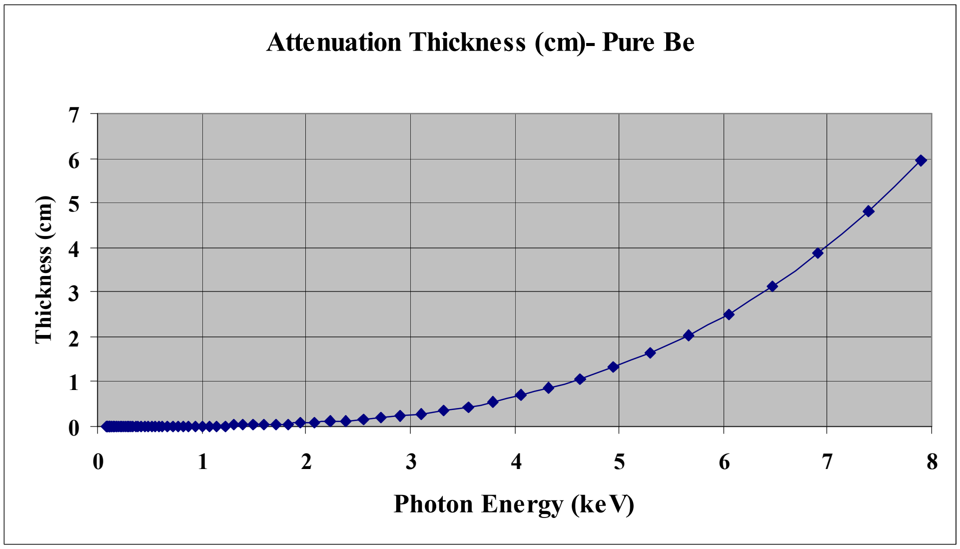

Fig. 2.2.1: Photon Energy versus Beryllium Thickness

Solid attenuators are required in the beam-line in order to meet the PRD requirement of attenuation range of up to 10,000 times at all x-ray energy levels from 826 eV to 8260 eV. At the 8.26 keV end of the spectrum, it is more difficult to get a gas to attenuate enough using a practical vacuum system and nitrogen. The baseline design uses nitrogen at 20 Torr, which only attenuates the beam by 13% at 8.26 keV, which isn't even close to the 10,000 times required. A modest amount of beryllium, around 2 inches thick, will attenuate the 8.26 keV beam more than 10,000 times. The attenuation requirement requires very little material at the low end and much more attenuation material at the high end. At the low end, using gas to attenuate makes sense because a low pressure gas has a very long attenuation length and can be varied in pressure to attain many attenuation levels. At low energies, it would be difficult to use solids as they attenuate too much in mechanically robust thicknesses. Solids begin to have useful attenuation levels at practical thicknesses for x-ray energies above 2000 eV.

In order to have the full range of energies covered and the full range of attenuations covered, both solid and gas attenuation will be utilized. In order to have the full range of attenuation levels covered, the thinnest solid attenuation slide must overlap the attenuation range of the gas attenuator.

The solid attenuator is conceived as having seven attenuation slides to have the required range of attenuation. The thinnest is set by having a good overlap with the gas attenuator. The thickest is set by having at total thickness of attenuation slides sufficient to attenuate 8.26 keV x-rays by a factor of 10,000. Each slide is twice as thick as the one before it. In the conceptual design, the slide thicknesses are 0.375, 0.75, 1.5, 3, 6, 12, and 24 mm. This combination has 128 available combinations from 0 to 47.625 mm in 0.375 mm increments.

Approach

The attenuation slides are required to have two states: in the beamline and clear of the field of spontaneous radiation defined by the fixed mask. Therefore, our baseline design uses a two state pneumatic actuator with sufficient throw to place the slide into the beamline and then withdraw it completely clear of the beamline.

The baseline actuator is UHV compatible. We have chosen and tested a Huntington UHV compatible actuator as our baseline actuator. It is designed to fail with the attenuation slide in for the case of the loss of air pressure. It uses micro-switches for limit switches to feedback that the slides is inserted or retracted. It is controlled via a 24 VDC solenoid.

The solid attenuation slides are going to reside in the main gas cell of the gas attenuator. The attenuation slides are much larger in cross section than the FEL. The slides are on the order of 30 mm wide, while the FEL is only 1 mm.

The slide holders will be designed to be open on the end so that no material but the beryllium of the attenuation slide crosses the path of the FEL at any time. The attenuation slides will have the best surface reasonably achievable in order to minimize the impact on the optical quality of the FEL.

The attenuation slides will be composed of the most uniform beryllium that meets other criteria, such as polishing, in order to have uniformity of attenuation.

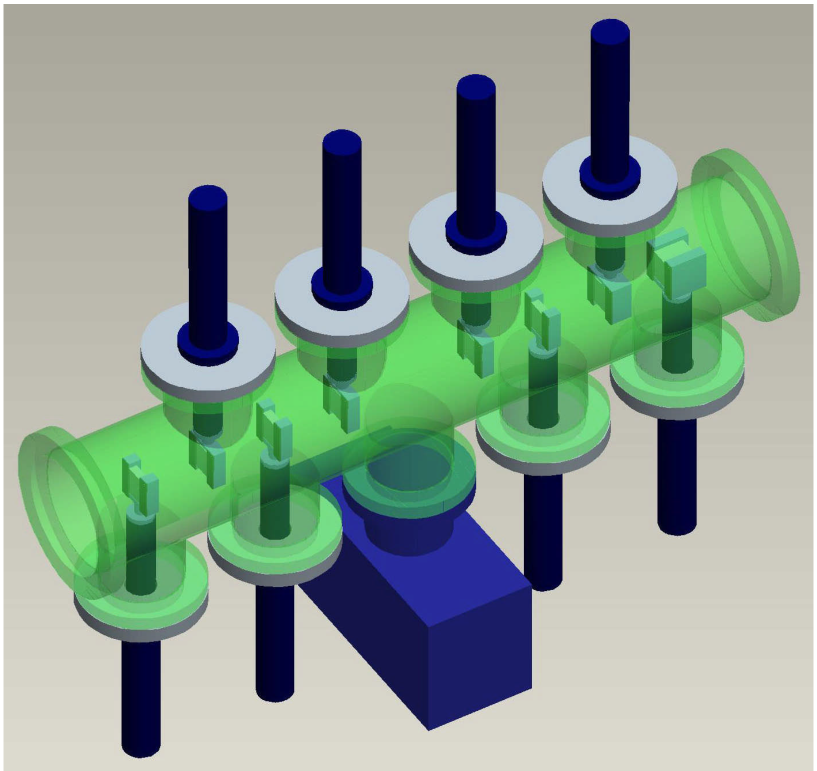

Figure 2.2.2: Solid Attenuator Concept

Solid Attenuator Actuator Prototype

The repeatability of attenuation of the x-ray FEL is a key requirement. Per the PRD for the system, the repeatability must be within 5% at the highest energy level (8.26 keV).

The baseline design employs seven stages in order to have a range that covers from how much the gas attenuator can attenuate. The thinnest stage is arrived at from a baseline for the gas attenuation maximum attenuation from 20 Torr of nitrogen in a 6 m gas cell. The thickest is set by the total attenuation required, taking the gas cell and thinner attenuation stages into account. With low attenuation at 8.26 keV from the gas cell, the thickest is basically half of the total thickness needed for maximum attenuation. The number of stages is set by the number of binary steps from the thinnest to the thickest

A rotation of the solid angle of the stages from the plane perpendicular to the FEL changes the thickness the FEL transverses. Changing the effective thickness changes the attenuation. In order to have 5% repeatability error for 10,000 times attenuation of 8.26 keV x-rays with Beryllium blocks that have 200 ppm Fe impurity, the blocks would have to be rotated 5.8 degrees.

The baseline actuator is a Huntington UHV compatible pneumatic actuator; model L-2271-4-LL-2D-SM-EX, with spring to extend.

A test stand was built with a test block on the end of the actuator that is sized to mimic the real load. The test stand was secured to a CMM in the LLNL precision measurement shop. The position of the face of the test block on the end of the actuator was determined by the CMM. The actuator was cycled 10 times. After each cycle, the coordinates five point on the face of the test block were measured. The measurements were made of the same five points every time. The measurements are in terms of change from the first position.

> The repeatability with respect to angle was calculated based on the change in location of the points of the face divided by the distance between them.
>
> The actuator repeated within 0.2 degree of rotation. The repeatability improved with cycling.
>
> This translates into a repeatability of attenuation within 0.04% at the highest attenuation level (the worst case) with all seven slides in.

The repeatability is over 100 times better than required. Therefore, it appears that the choice of actuator for the Solid Attenuator is sound. Test arrangements are shown in the following pictures (Fig. 2.2.3-6).

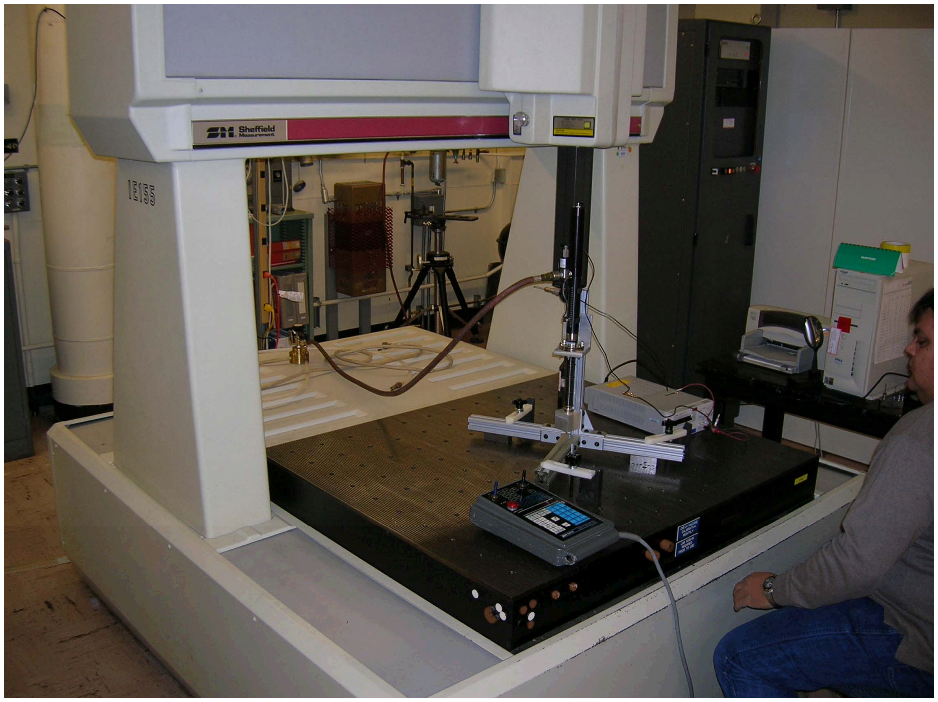

Fig. 2.2.3: Actuator Test on CMM

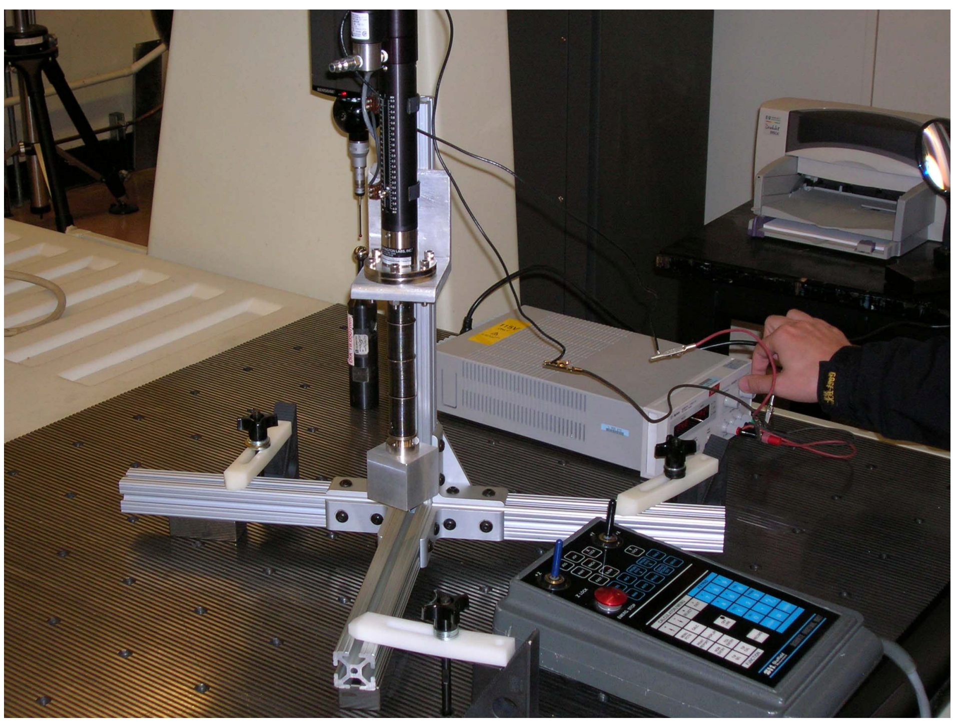

Fig. 2.2.4: Actuator Test Stand

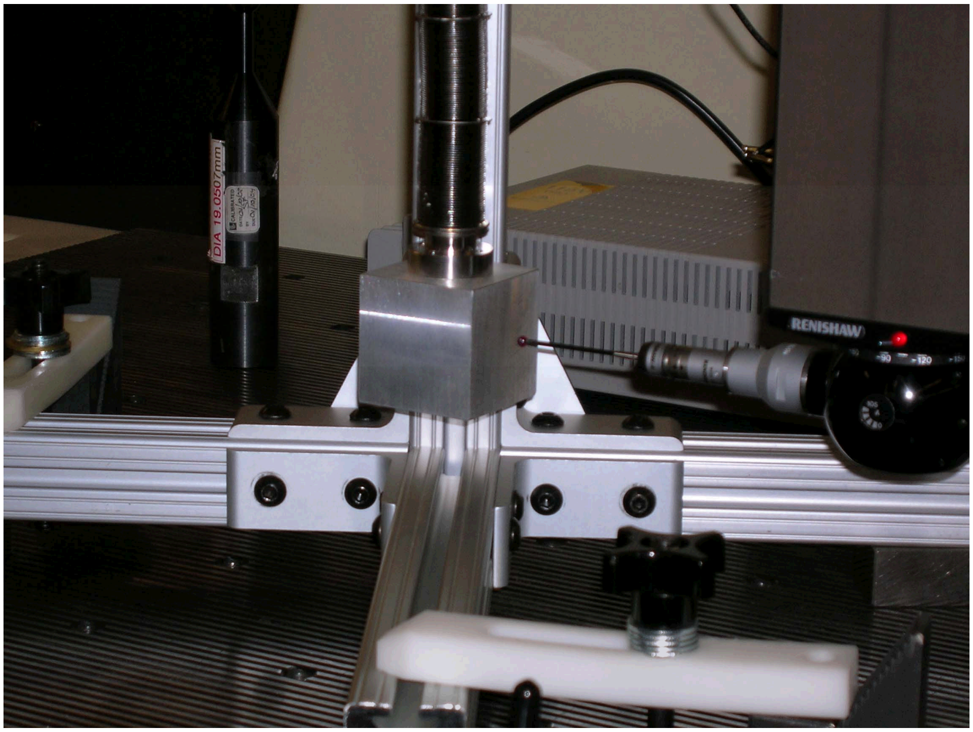

Fig. 2.2.5: CMM Probe on Test Block

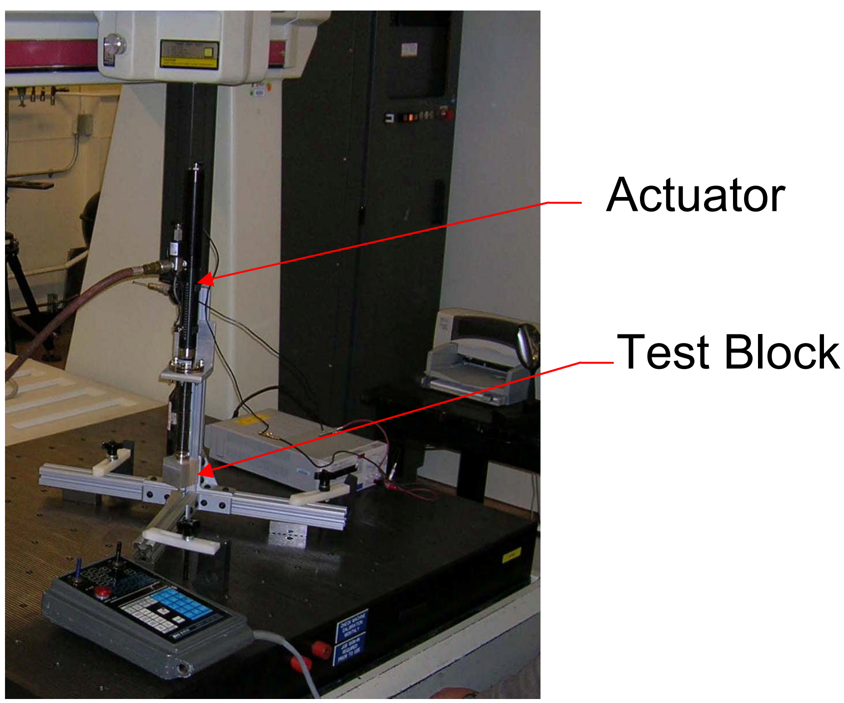

Figure 2.2.6: Solid Attenuation Actuator Repeatability Test

2.3 Gas Attenuation

N_2 gas is considered first. For the 6-m chamber design the required pressures are plotted in Fig. 2.3.1 for both 1.95 KeV and 1 KeV. This result specifies the N_2 pressure needed in the gas chamber. The plot is based on NIST X-Ray Form Factor, Attenuation, Scattering Tables [2].

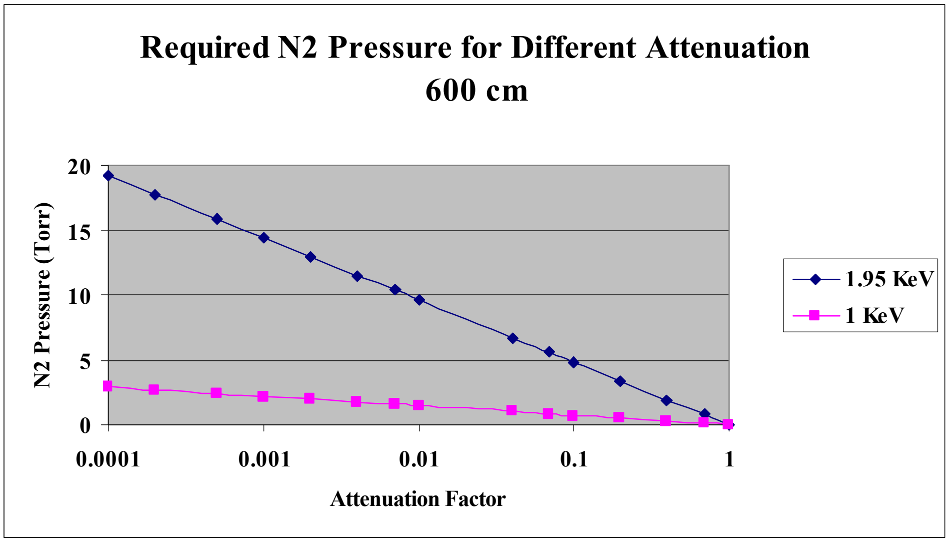

Fig. 2.3.1: N_2 attenuation vs. Pressure for 6-m Gas Chamber

The alternative gas is Ar, and its pressure vs. photon energy for 600-cm chamber with 10,000 attenuation factor is shown in Fig. 2.3.2 below.

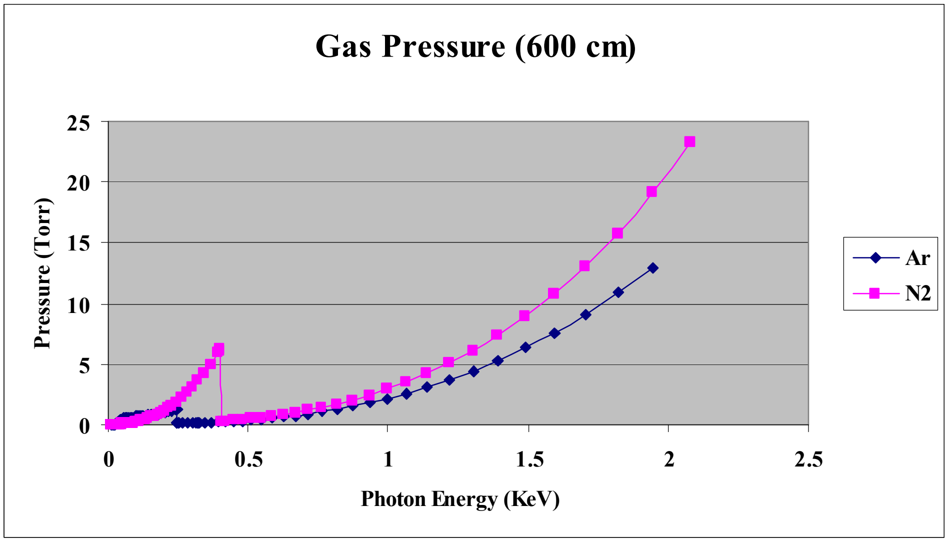

Fig. 2.3.2: N_2 and Ar Pressure vs. Photon Energy for 6-m Gas Chamber and Attenuation factor of 10,000

One can see that required Ar pressure for 1.95 KeV photon is about 13 Torr as compared to 19 Torr required for N_2 gas. More importantly, as shown in Fig. 2.3.3, Ar would provide very efficient attenuation beyond 3.2 KeV. In fact, 55-Torr Ar gas in a 6-m chamber can result in attenuation factor 10000 for 8 KeV photon beam.

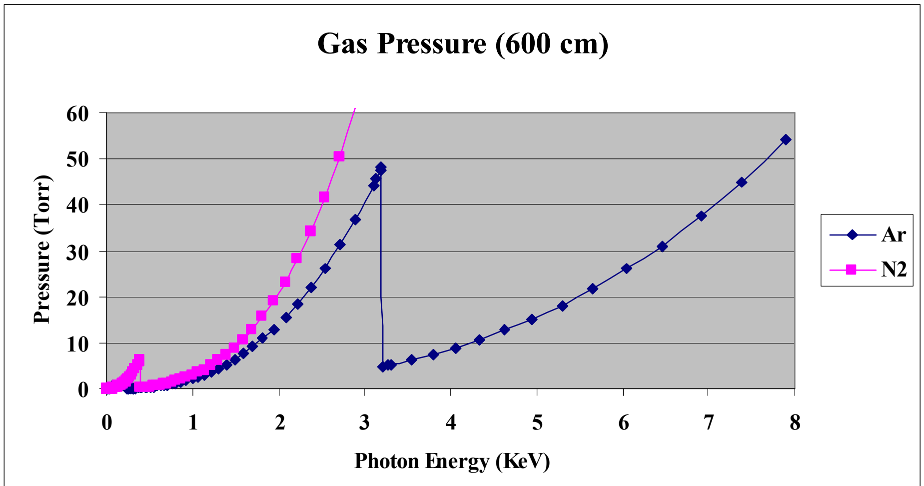

Fig. 2.3.3: N_2 and Ar Pressure vs. Photon Energy for 6-m Gas Chamber and Attenuation factor of 10,000

2.4 Baseline Approach

A beryllium disk will be welded in the face of the gate valve because it is transparent to high energy spontaneous and allows alignment of the aperture hole using WFOVDI camera in FEE. The gate valve can remove the beryllium window when gas attenuator is not in use.

X-ray Energy	Gas (N_2) Pressure (Torr)	Solid (Be) Thickness (um)	Design
827	1.7	46.5	Gas
2000	19.5	672.0	Gas
4000	152.5	5962.5	Solid
6000	527.8	22087.8	Solid
8000	1292.6	56579.1	Solid

However, there are several technical issues on this approach that cause concerns, as summarized in the following table.

System	Issue	Description	Alternative
Gas	Accuracy and Repeatability	< 1%	Relaxed to 5%
	Control	Attenuation level adjustment time < seconds	Relaxed to minutes
Aperture	Formation of Be_4N		Replaced with Argon gas

2.5 Ar Gas -Solid Combined Approach

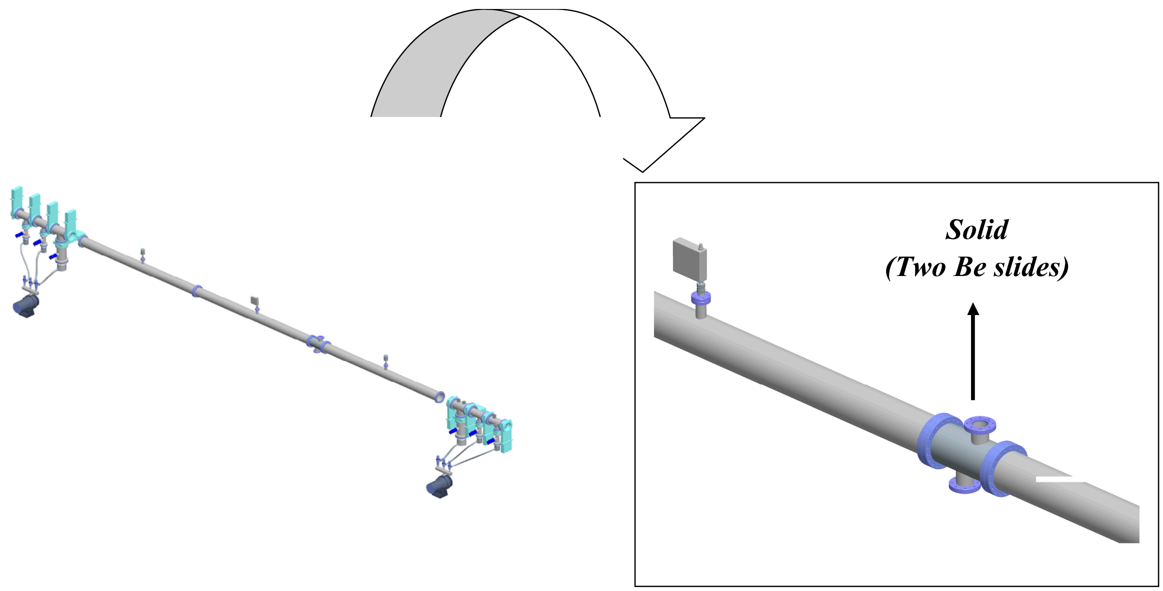

3 Vacuum System Design and Analysis

3.1 Gas Flow Conditions

The design goal is to maintain stable vacuum in the range of 10-50 Torr within the volume of the gas attenuator chamber, while gradually lowering the pressure to 3×10^{-6} Torr at the end ports. To be conservative, viscous (x>MP) and mixed flows (x~MP) are considered for the calculation of flow conductance (Fig. 3.1.1).

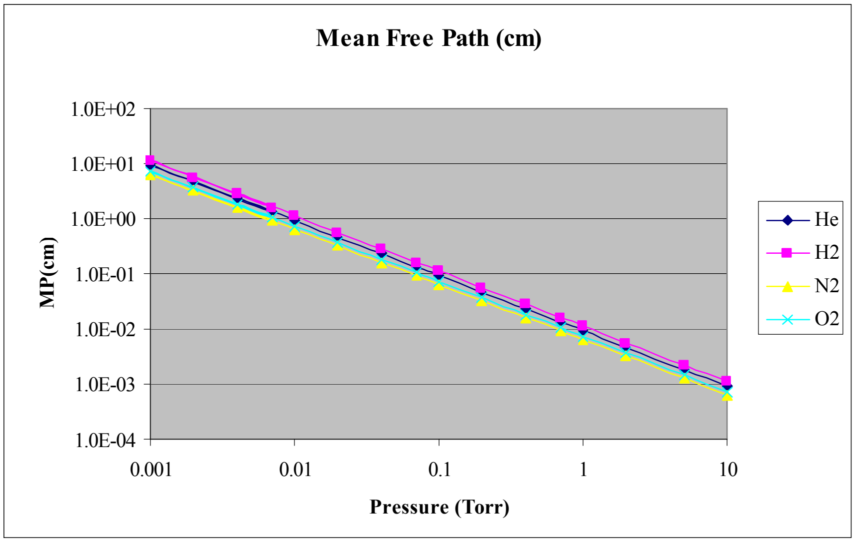

Fig. 3.1.1: Mean Free Path as a function of Pressure

3.2 Passive Pumping System Approach

We started with the 4-port configuration as shown in the upper portion of Fig. 3.2.1. However, it turned out that the high pressure gradients and hence excessive pumping would be needed to satisfy the end cell vacuum requirements. We then proceeded with the 6-port configuration as shown in the lower portion of Fig. 3.2.1.

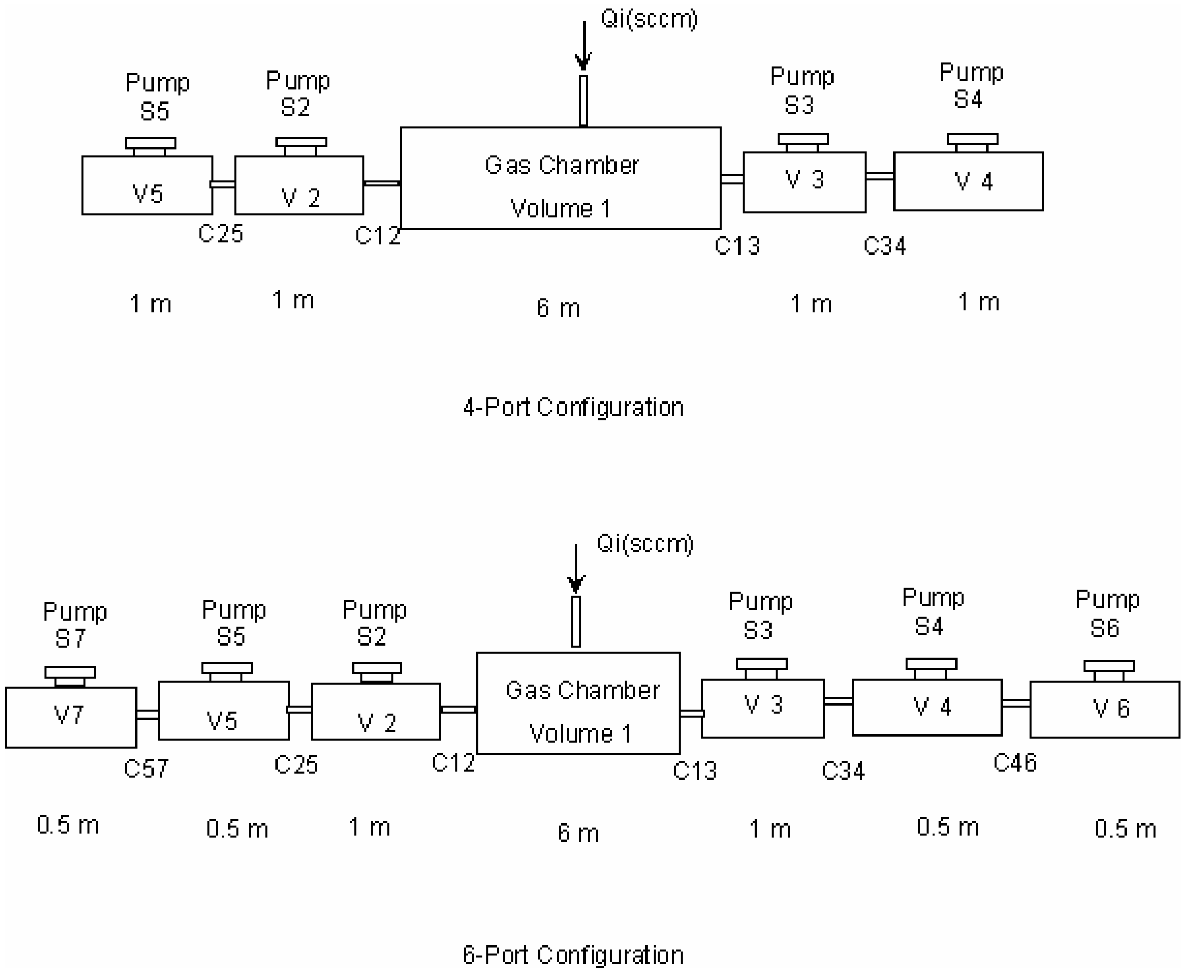

Fig 3.2.1: Four Port and Six Port Configurations

The preliminary system design parameters are shown in Table 3.2.1.

Parameter	Unit	Value
Configuration		Passive 6-port B
Total Length	m	10
Gas Chamber Length Diameter	m m	6.0 0.15
Port 2 &3 Length Diameter	m m	1 0.15
Port 4 &5 Length Diameter	m m	0.5 0.125
Port 6 &7 Length Diameter	m m	0.5 0.125
Total Equivalent Combined Pumping Speed (turbo+scroll)	L/s	720
Gas		N_2
Chamber Pressure for 10^4 Attenuation	Torr	19
Max Gas Flow	sccm	5400
1^{st} Port Pressure (V_2)	Torr	1.8
Last Port Pressure (V_7)	Torr	4.2×10^{-7}

Table 3.2.1: System Major Design Parameters

The complete system diagram is illustrated in Fig. 3.2.2 below:

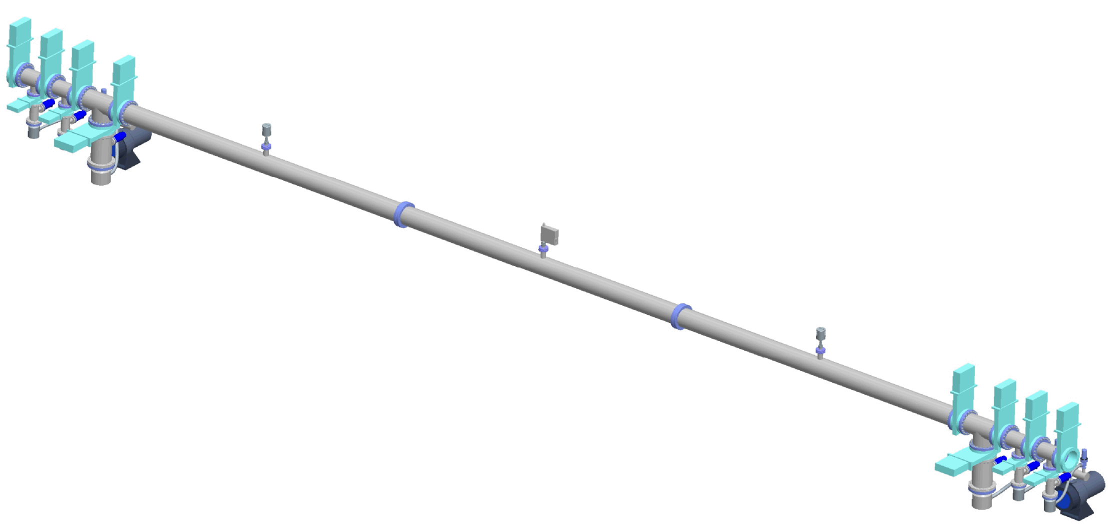

Fig. 3.2.2: Gas Attenuator Configuration

3.3 Analysis Model

As shown in Fig. 3.2.1, the vacuum system is divided into 7 volumes and their pressures are described by the following gas-load equations:

$$V_1 \frac{dP_1}{dt} = Q_i + Q_1 + C_{12}(P_2 - P_1) + C_{13}(P_3 - P_1) \tag{1}$$

$$V_2 \frac{dP_2}{dt} = Q_2 - S_2 P_2 + C_{25}(P_5 - P_2) + C_{12}(P_1 - P_2) \tag{2}$$

$$V_3 \frac{dP_3}{dt} = Q_3 - S_3 P_3 + C_{13}(P_1 - P_3) + C_{43}(P_4 - P_3) \tag{3}$$

$$V_4 \frac{dP_4}{dt} = Q_4 - S_4 P_4 + C_{34}(P_3 - P_4) + C_{46}(P_6 - P_4) \tag{4}$$

$$V_5 \frac{dP_5}{dt} = Q_5 - S_5 P_5 + C_{25}(P_2 - P_5) + C_{57}(P_7 - P_5) \tag{5}$$

$$V_6 \frac{dP_6}{dt} = Q_6 - S_6 P_6 + C_{46}(P_6 - P_4) \tag{6}$$

$$V_7 \frac{dP_7}{dt} = Q_7 - S_7 P_7 + C_{57}(P_5 - P_7) \tag{7}$$

where C_{jk} coupling conductance through the nominal 3-mm aperture (L/s)
S_j the effective pumping speed (L/s see)
Q_j outgassing rate (T-L/sec) for each volume
V_j voloume (L)
P_j pressure (Torr) in each volume
Q_i injected gas (T-L/s or sccm)

Calculation of Coupling Conductances

In above equations, $C_{jk} = C_{kj}$ is the coupling conductance. The calculation of C_{12} and C_{13} is based on intermediate flow [3], while the rest of them are assumed to be in molecular flow regime.

Roughing Pumping Speed

Since the pumping speed of a mechanical pump is strongly dependent on the pressure, the model implements the exact pump speed of a Varian TriScroll 600 pump as a function of pressure as shown in Fig. 3.3.1 below.

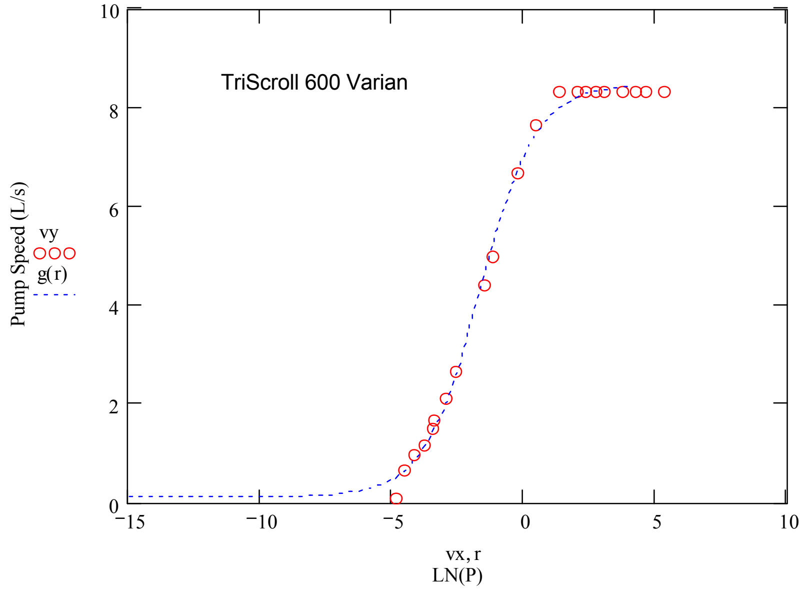

$$S(P) = 4.298 + 4.177 \tanh(0.469\, LN(P))$$

Fig. 3.3.1: Pump Speed as a function of pressure for a 600-L/min Scroll Pump.

<u>Turbo Pumping Speed</u>

Since the speed of a turbo pump is also strongly dependent on the pressure, the model implements the exact pump speed of a Varian turbo pump as a function of pressure as shown in Fig. 3.3.2 below.

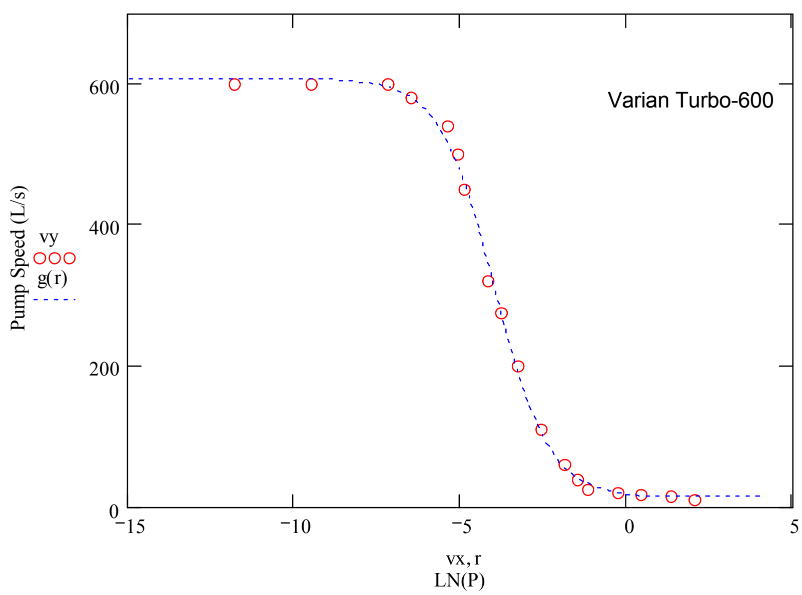

$$S(P) = 310.673 - 26.442 \tanh(0.617\, LN(P))$$

Fig. 3.3.2: Pump Speed as a function of pressure for a 600-L/s Turbo Pump.

Analyses are performed for a series of vacuum operation modes.

1. Roughing Down from 760 Torr

It is assumed the evacuation starts at atmosphere pressure of 760 Torr. The total volume is about 180 liters. The calculated result of pressure decay with time is shown in Fig. 3.3.1. The operating conditions are listed in Table 3.3.1.

System	**Component**	**Values or condition**
Initial System Pressure	P_1 ,P_2 ,P_3 P_4 ,P_5 ,P_6 P_7	760 Torr
All valves		Open position
Vacuum Pumps	S2 & S3 (Scroll)	Max 30 L/s each
	S4 & S5 (Turbo) S6 & S7 (Turbo)	Max. 300 L/s each Max 300 L/s each
Injected gas	Qi	0 (valve closed)

Table 3.3.1: Operation Condition for Roughing Down

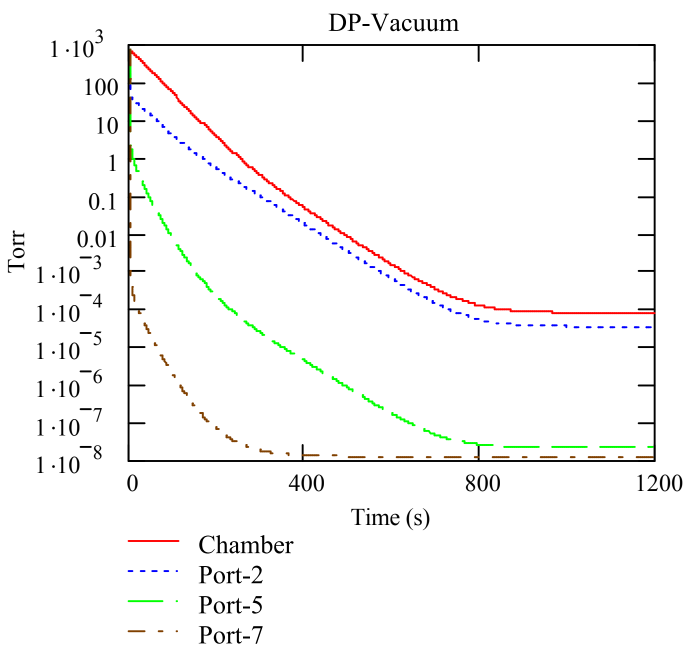

Fig. 3.3.1: Pump-Down Curve

2. Normal Operation with Injected Gas

The operating conditions are listed in Table 3.3.2.

System	Component	Values or condition
Initial System Pressures	P_1 (Gas Chamber) P_2 P_3 P_4 P_5 P_6 P_7	7.94×10^{-5} Torr 3.43×10^{-5} Torr 3.43×10^{-5} Torr 2.10×10^{-8} Torr 2.10×10^{-8} Torr 1.20×10^{-8} Torr 1.20×10^{-8} Torr
All pump valves		Open
Vacuum Pumps	S2 & S3 (Scroll) S4 & S5 (Turbo) S6 & S7 (Turbo)	Max 30 L/s each Max. 300 L/s each Max 300 L/s each
Injected gas	Qi	5368 sccm on @ t= 1sec

Table 3.3.2 Operation Condition for Effective Pump Speed Test

The N_2 gas injection sequence is illustrated in Fig. 3.3.2, where the peak value is 82 T-L/S (6474 sccm).

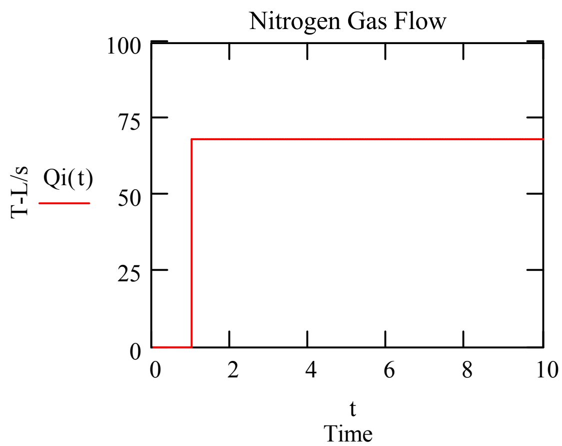

Fig. 3.3.2: Opening sequence of N_2 gas flow

The pressure rise in each volume for the first 5 seconds is shown in Fig. 3.3.3.

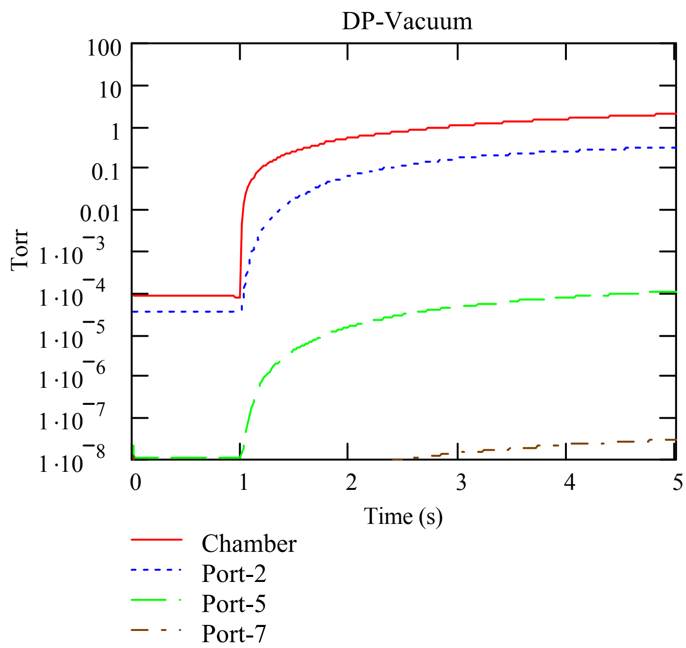

Fig. 3.3.3: Pressure rise in the system for t=0 to 5 sec.

The same pressure history is also plotted for t= 150 second in Fig. 3.3.4.

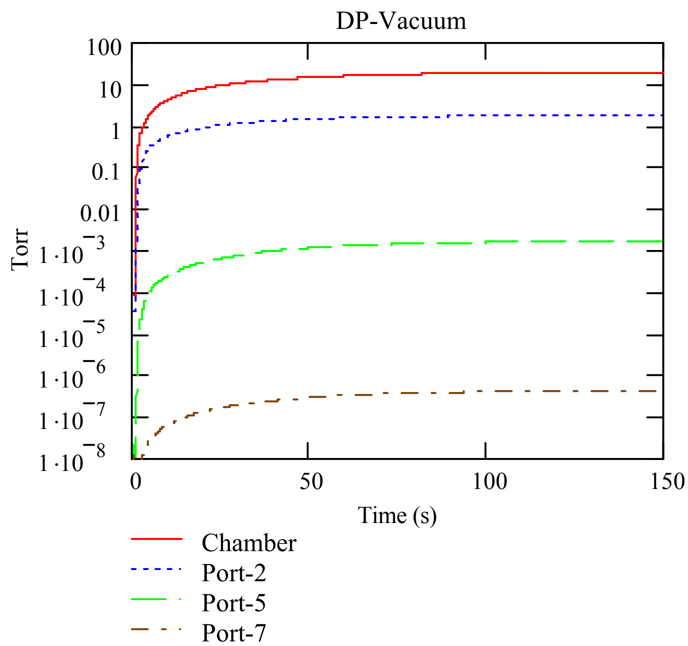

Fig. 3.3.4: Pressure rise in the system for t=0 to 150 sec

The pressure rise in the gas chamber is plotted separately in Fig. 3.3.5.

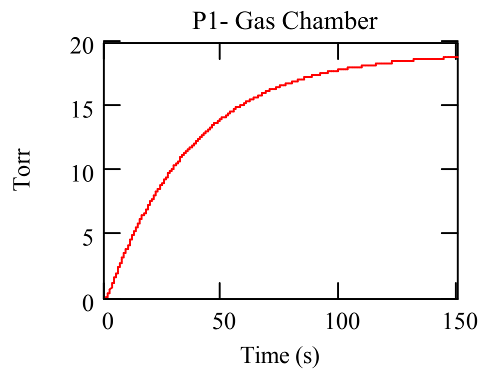

Fig. 3.3.5: Pressure rise in the gas chamber resulted from the injected N_2 gas

It is clearly shown that 19 Torr gas pressure can reach steady state in about 150 seconds.

3.4 Prototype Model

In order to verify the gas flow calculation and validate the design, we have prepared a prototype plan. The system configuration diagram is shown in Fig. 3.4.1.

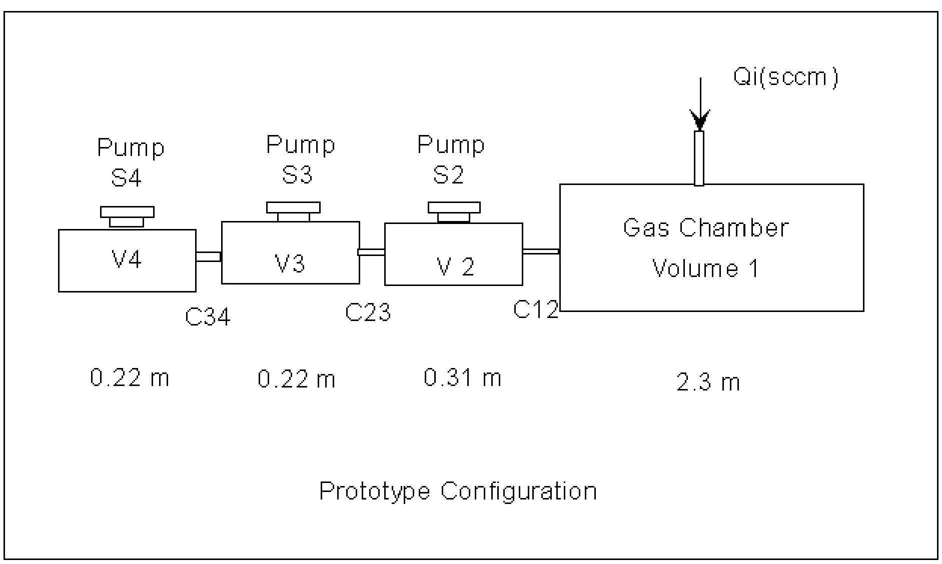

Fig. 3.4.1: Prototype Configuration

The complete system arrangement is shown in Fig. 3.4.2.

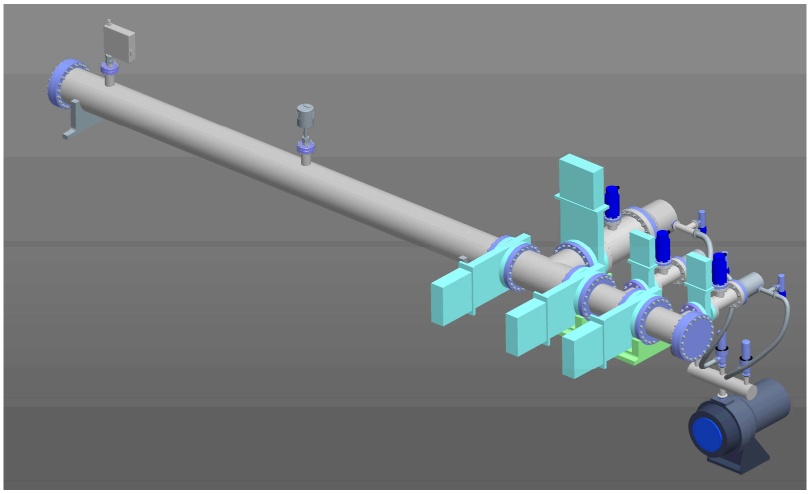

Fig. 3.4.2 Prototype Gas Attenuator Arrangement

The design parameters are listed in Table 3.4.1.

Parameter		Unit	Value
Configuration			Passive 3-port
Total Length		m	3.27
Gas Chamber	Length	m	2.53
	Diameter	m	0.15
Port 2	Length	m	0.31
	Diameter	m	0.15
Port 3	Length	m	0.22
	Diameter	m	0.125
Port 4	Length	m	0.22
	Diameter	m	0.125
Vacuum Pumps		L/s	
Turbo-1			300
Turbo-2			75
Turbo-3			75
Scroll			20
Gas			N_2& Ar
Chamber Pressure for 10^4 Attenuation		Torr	20
Max Gas Flow		sccm	3268
1st Port Pressure (V_2)		Torr	0.32
Last Port Pressure (V_7)		Torr	1.0×10^{-6}

4 Mechanical Design

4.1 General Description

The system layout has been shown in Chapter 3. Fig. 4.1.1 illustrates the arrangement of the transition stage.

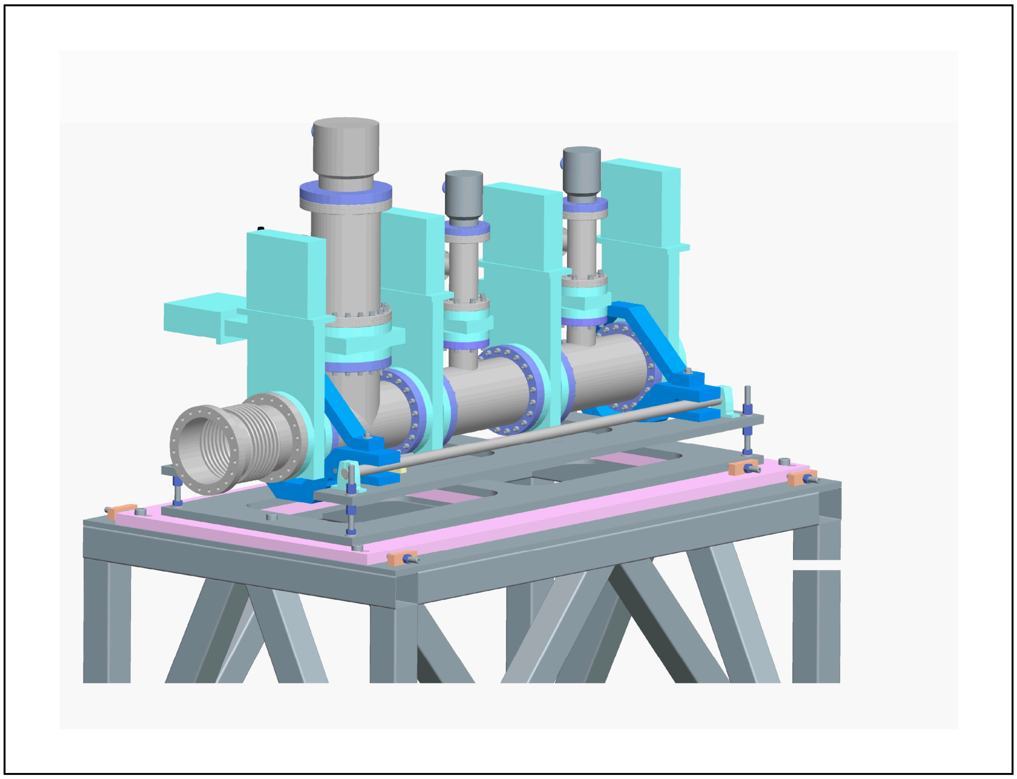

Fig. 4.1.1: Conceptual Layout of Pumps for Ports 3, 4 and 6

4.2 Seismic Analyses – Structural

The main analysis tools used were the SAP 2000 version 9.1.7 program and the HILTI PROFIS anchoring analysis program version 1.5. SAP 2000 is a highly capable structural analysis program. It gives the fundamental modes of the structure, deflections under load, and analyzes the structure, both aluminum and steel, per the appropriate design codes, Aluminum Association Allowable Stress Design (AA ASD) and American Institute of Steel Construction's Load Resistance Factor Design (AISC LRFD), and gives the reactions at the structure's restraints.

The seismic loads are per the SLAC document, "Specification for Seismic Design of Buildings, Structures, Equipment, and Systems at the Stanford Linear Accelerator Center" dated December 4, 2000. The SLAC document yields a load of 1.5g's in the horizontal plane and 1.15g's vertically for a structure with 2% damping with a natural frequency of 20 Hz. Structures with 2% damping are typically welded, while structures with 5% damping are usually bolted. The seismic response curve is about 25% higher for 2% damping. The use of 2% damping is therefore conservative in this case, but not overly so. The first natural frequency being around 20 Hz was confirmed by SAP 2000.

5 Instrumentation and Control

5.1 Introduction

The design of the instrumentation and control system for the LCLS XTOD attenuator system will be based on the design of the LCLS XTOD tunnel vacuum system. The control system's basic design is to have a Programmable Logic Controller (PLC) controlling the vacuum pumps and gate valves. The PLC will be connected to a network which will have EPICS I/O Controllers (IOCs) that will provide the data to a user interface in a client server model. The PLC will monitor the status of the vacuum pumps and vacuum setpoints from the vacuum gauge controllers and use interlocks generated from the PLC's logic to ensure proper operation of the vacuum system. In the event of a vacuum system malfunction, interlocks will be available to the Machine Protection System to safely shutdown the system.

The pressure of the gas attenuator chamber will be controlled by an electronic pressure controller. These are commercially available and they typically have a capacitance manometer to monitor the pressure independent of the gas species, a mass flow meter, a normally closed proportioning control valve and a closed loop control system all integrated into one unit.

The design of the attenuator in the six port configuration uses scroll and turbo pumps in ports 2, 3, 4, 5, 6 and 7. The final selection of the pump speeds in each of the ports will be made based on the results of the prototype.

During a power failure, the gas attenuator vacuum system will shut down. When power is restored, the PLC will reboot, but will not restart the gas attenuator vacuum system. The state of the system will have to be determined by an operator who will then use the EPICS control system to command the PLC to restart the vacuum pumps and open gate valves. Once the vacuum system has stabilized, the operator can resume gas flow into the gas attenuator.

The gas attenuator system will be in full compliance with LCLS standards for hardware, software and safety.

5.2 Vacuum Controls

The control system for the gas attenuator will consist of a PLC that will be connected via a network to the global control system, EPICS. The PLC will execute its ladder logic software in a continuous loop, evaluating the status of the gas attenuator vacuum system. Based on the ladder logic and the status of the vacuum system, the PLC can automatically close a valve or shutdown a pump. The PLC can not automatically open a valve or start a pump, such an operation must be done by an operator using EPICS. Interlock logic within the PLC will prevent the operator from selecting an improper valve or pump operation.

The PLC can be operated in a stand-alone mode by using a PC running the PLC software development environment to open a valve or start a pump. This mode will only be used for initial testing and commissioning and only by personnel experienced with the PLC software development environment and vacuum systems. This mode may also be used after commissioning in the event EPICS is not running and only when an urgent vacuum system problem must be diagnosed.

LCLS has decided to standardize on the Allen-Bradley ControlLogix family of PLCs and associated hardware and software. This will utilize the experience and software that SNS has developed with the ControlLogix PLCs in the EPICS environment. Allen-Bradley provides a large software development environment (i.e. RSLogix, RSNetWorx, RSLinx) that runs under Windows and is used to configure and program the ControlLogix PLC. A block diagram of the gas attenuator is shown in Figure 5.2.1.

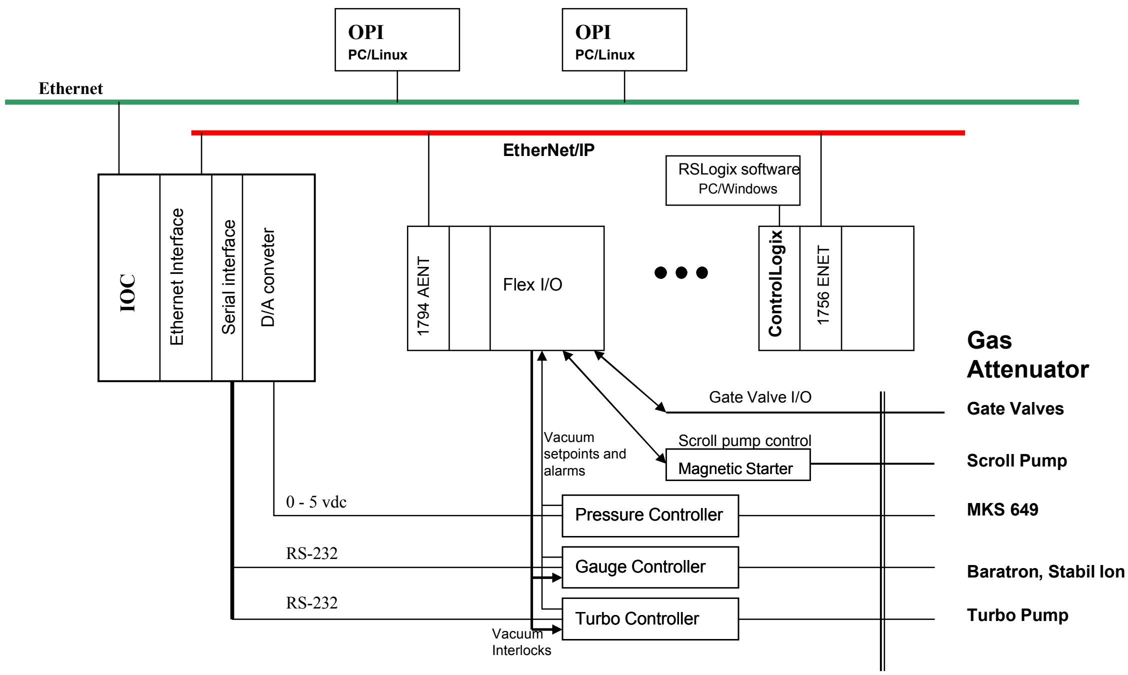

Figure 5.2.1: Block Diagram of the Gas Attenuator Vacuum Control System

The gas attenuator system will use the Allen-Bradley modular distributed I/O system known as Flex I/O. Flex I/O consists of a family of I/O modules with each module having its own terminal strip and communications backplane. The I/O modules can be mounted on DIN rails in a local rack or cabinet.

A network module using the Ethernet Industrial Protocol (EtherNet/IP) is then added to the DIN rail and connected to the I/O modules' communication backplane, allowing the I/O modules to communicate their data to the PLC via EtherNet/IP. Flex I/O requires only local wiring to the devices, eliminating long and complex wiring runs back to the PLC.

There will be vacuum interlocks to protect the pumps and other vacuum systems upstream and downstream of the gas attenuator. These general-purpose interlocks will be provided by the PLC via a Flex I/O digital output module and will be used for such things as interlocks for isolation gate valves between sections controlled by a different PLC. There will also be software interlocks that will be generated by the PLC or the IOC. These interlocks will be mainly used by EPICS to control high level functions for gas flow in the attenuator.

5.3 Instrumentation

The measurement of the vacuum pressure in the gas attenuator chamber is critical. A capacitance manometer from MKS, better know by the trade name "baratron" has been selected. The standard unit which operates at ambient temperature has an accuracy of 0.25% of reading. If additional accuracy is desired, a temperature controlled unit is available that has an accuracy of 0.12% of reading. If even higher accuracy is required, a high accuracy, temperature controlled series is available with an optional calibration to 0.05% of reading.

Capacitance manometers measure the true pressure defined as force per unit area by measuring the change in capacitance between the metal inlet diaphragm and an adjacent, fixed electrode. Because the diaphragm is measuring the force per unit area, the measurement is independent of gas species. This will be important if the gas in the attenuator is switched from nitrogen to argon. Other gauges such as convection enhanced piranis are non-linear with different gas species in the typical operating pressure range of the gas attenuator.

For the prototype, a MKS type 649 electronic pressure controller has been selected. The pressure control accuracy is $\pm$0.2% of full scale and a time response of 1.0 seconds excluding the overall vacuum system time constant. The type 649 can flow 5,000 sccm of nitrogen, which should be sufficient for operating the prototype at 20 Torr. If higher attenuation levels are desired, then a master-slave type configuration will be required for the higher flows rates needed to operate the gas attenuator above 20 Torr. The master-slave configuration closed loop control parameters can be tuned on the prototype.

The gas supply for the type 649 pressure controller will be equipped with a small accumulator and a pressure transducer. By using an accumulator, if the pressure begins to drop indicating a loss of the gas supply, an interlock should give sufficient warning to the Machine Protection System that the gas attenuation is going to be unstable.

Several platinum RTDs will be used to measure the temperature of the prototype gas attenuator chamber. This will determine if a temperature gradient exists due to the gas flow. If necessary, the temperature of the actual gas attenuator can be measured and recorded along with the gas pressure.

To verify the calculations of the model, accurate ion gauges are required for the prototype in ports 3 and 4. This will determine if the turbos have pumped out ports 3 and 4 to a sufficient vacuum condition to meet the interface requirements. The Granville-Phillips Stabil-Ion gauges are specifically designed to eliminate the common sources of measurement error found in a typical hot filament nude ion gauge. In addition the model 370 Stabil-Ion gauges are individually calibrated at the factory and are shipped with a calibration memory model that can be downloaded into the gauge controller to provide 3% accuracy.

Once the calculations of the model have been verified and if there is sufficient margin, the accuracy of the Stabil-Ion would not be needed in the gas attenuator. The preliminary design calls for cold cathode ion gauges in ports 4, 5, 6 and 7. Ports 6 and 7 interface to the beamline.

The ion gauge that has been selected is a MKS Type 422 inverted magnetron cold cathode gauge. The Type 422 is identical to the standard Type 421 cold cathode gauge except that is uses LEMO type connectors which are bakeable to 250 C and are radiation resistant. The accuracy is 25%, which is significantly less than the Stabil-Ion.

Convection enhanced pirani gauges will be used in ports 2 and 3, on each side of the gas attenuator section if nitrogen is the primary gas. Ports 2 and 3 have the highest gas loads, so it is essential that there are gauges to measure the pressure in these ports to insure that the pumps are operating normally. The convection enhanced pirani gauge will also be useful to monitor the vacuum system during pumpdown from atmosphere. The convection enhanced pirani gauge was selected because it is more accurate at the higher pressures than a thermocouple gauge or a basic pirani gauge since it has a temperature compensated heat sensor and can measure convection current. The gauge that has been selected is the MKS Type 317.

However, if argon is used, the convection enhanced pirani gauges should be replaced with capacitance manometers due to the non-linear response of the convection enhanced pirani gauge to gases other than nitrogen.

5.4 Software

One of the primary goals of the vacuum control system software will be full compatibility with the global control system EPICS. The Allen-Bradley ControlLogix PLC has been selected for the vacuum control system. The use of the ControlLogix PLCs will capitalize on the software that was developed for EPICS at SNS. A typical EPICS Control System block diagram is illustrated in Fig. 5.4.1.

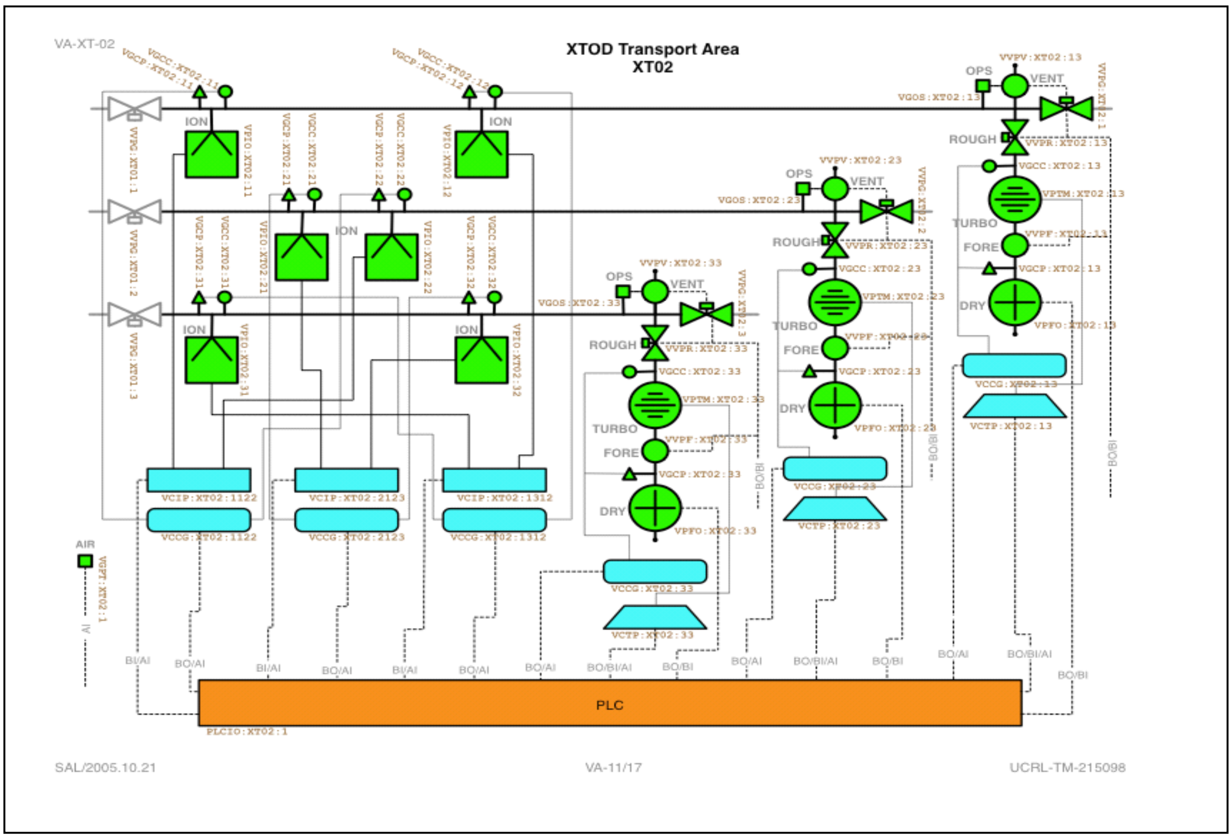

Figure 5.4.1: EPICS System Block Diagram

The gas attenuator vacuum control system will use ladder logic in the PLCs. Ladder logic describes the sequence of switch closures, interlocks and process control setpoints that have to be executed in order to energize a valve or start a vacuum pump. The start up and operation of any vacuum system will in general have the same basic sequence of switch closures, interlocks and setpoints and therefore the ladder logic can become part of a toolkit of software that can be re-used.

The ladder logic is solved in a specific sequential order and coils from one function are used as interlocks in the next function. The ladder logic structure is in essence, a flow chart. For example, to open the a foreline valve to a turbo pump, the scroll pump backing the turbo must have been started in the previous function and must be currently running. If the scroll pump were to experience a thermal overload and shut down the foreline valve be forced to close too.

For example, there will be five basic steps that must be executed in the proper order to bring the gas attenuator vacuum system up to an operational status ready for gas flow. They are:

1. Start the scroll pump
2. Open the foreline valve to the turbo
3. If conditions permit, open the gate valve to the gas attenuator chamber and start roughing down the chamber
4. If conditions permit, start the turbo
5. When the vacuum is stable, start the gas flow

These basic steps is a simple example of how the ladder logic software and will be used to operate the LCLS Gas Attenuator vacuum system.

5.5 Failure Mode Analysis

An analysis of possible failure modes in the vacuum system are show in the table 5.5.1. Table 5.5.1 shows various failure modes, an empirical (i.e. low, med, high) probability of each failure mode, the most likely symptom that would be observed and the PLC response to the failure. With the experience gained from operating the prototype, the failure modes and the PLC response maybe modified.

Table 5.5.1 Failure Analysis and Control System Response for Gas Attenuator

System	Failure or Condition	Probability	Symptom	PLC Response/Interlock
Scroll and Turbo Pumps	Scroll pump head failure	Low/med - failures are usually due to lack of periodic maintenance (every 10,000 hours)	Low base pressure Low pump speed	Pirani gauge monitoring foreline pressure or pirani or baratron gauge monitoring ports 2 & 3 PLC interlock will shutdown scroll pump PLC interlock will shutdown turbo PLC interlock will close turbo gate valve PLC interlock will shutdown gas flow PLC sends scroll pump fault message to EPICS
	Scroll pump motor failure	Low - motor bearing or winding failure uncommon	High motor current or windings open or short	Motor control circuit (or circuit breaker) will shutdown the scroll pump and send a fault signal to the PLC PLC interlock will shutdown turbo PLC interlock will close turbo gate valve PLC interlock will shutdown gas flow PLC sends scroll pump fault message to EPICS
	Scroll pump gas load too high	med - vacuum system leak or contamination or gas flow too high in gas attenuator chamber	High motor current	System will not pump down, PLC will timeout, stop pump, send timeout message to EPICS Scroll pump will overheat, motor control circuit will shutdown the scroll pump and send fault signal to PLC PLC interlock will shutdown gas flow PLC interlock will shutdown turbo PLC interlock will close turbo gate valve to protect scroll pump PLC sends scroll pump fault message to EPICS

System	Failure or Condition	Probability	Symptom	PLC Response/Interlock
Scroll and Turbo Pumps (Cont.)	Turbo pump bearing failure	Low - modern ceramic bearings are very reliable	High motor temp High motor current	Turbo controller will provide safe shutdown and send fault signal to PLC PLC interlock will shutdown gas flow PLC interlock will close turbo gate valve PLC sends turbo fault message to EPICS
	Turbo rotor crash	Low - Unless turbo ingests foreign object or is subject to multiple atmospheric vents while operating at full speed	Sudden drop in RPMs	Turbo controller will shutdown pump and send fault signal to PLC PLC interlock will shutdown gas flow PLC interlock will close turbo gate valve PLC sends turbo fault message to EPICS
	Turbo gas load too high	Low/med - vacuum system leak or contamination or gas flow too high in gas attenuator chamber	High motor current High motor temp Low RPMs	Turbo controller will provide safe shutdown and send fault signal to PLC PLC interlock will shutdown gas flow PLC interlock will close turbo gate valve to protect turbo PLC sends turbo fault message to EPICS
Electronic pressure controller	Gas supply empty or pressure too low to regulate	Low/med – pressure transducer on supply will alert when supply is too low	Pressure drop in gas attenuator chamber	Pressure transducer will provide signal to PLC PLC interlock will alert operators that supply is low PLC interlock to MPS will dump beam if pressure is critically low
	Malfunction in electronic pressure controller	Low – unit is widely used in semiconductor industry	Pressure in attenuator unstable	Baratrons monitoring pressure in attenuator will have an interlock window around pressure setpoint PLC interlock to MPS will dump beam if pressure is outside setpoint window

6 Environmental, Safety, and Health

6.1 Design Details

The attenuator system will be designed at LLNL based on calculations and operation of prototype system. During this process, the system design will be continually evaluated for safety in every phase of LCLS work, including design, transportation, installation, testing, operation, and maintenance. LLNL IWS #12920 “LCLS Prototype Attenuator System” was prepared and approved.

6.2 ES&H Policy

All work will be done in accordance with LLNL ES&H policies. These policies are addressed in the LLNL “Health and Safety Manual” and the “Environmental Protection Handbook”. Furthermore, LLNL ES&H policies implement U.S. Department of Energy orders to comply with all local, state, and federal regulations. These policies are carried out in accordance with LLNL’s Integrated Safety Management program using and Integrated Worksheet. Furthermore, all work performed by LLNL employees at SLAC will be in accordance with SLAC safety rules, and all LLNL safety documentation for LCLS will be written with the goal of meeting SLAC documentation requirements.

6.3 Design Details & Potential Hazards

During certain maintenance operations, some or all of the sections of the attenuator vacuum system may be purged with a positive pressure of dry N_2 gas to prevent contamination from the atmosphere from reaching the interior surfaces of the vacuum system. The design will address the pressure safety of the attenuator system. Each section will have a valve to vent the system to atmosphere pressure. It is recommended that clean, dry nitrogen be used to vent the system and to continuously purge the system while it is open so that the interior surfaces of the vacuum remain as clean and moisture free as possible. A low pressure regulator is required to prevent overpressurization of the system. Burst discs of the proper relief pressure will be installed on all sections in the event of overpressurization.

Since nitrogen and argon displaces oxygen, the facility will have to determine if a confined space exists and provide the appropriate controls for such a hazard. Other than the pressure safety of the vacuum vessels, the operation of a vacuum system poses few hazards. The obvious hazards are generally associated with the operation of the vacuum pumps and electromechanical equipment such as valves.

The turbomolecular pump controller outputs a 56 VAC, 3 phase, 700 Hz signal to the pump. The turbomolecular pump controller can detect an open circuit and will not output a voltage under such a condition. There is also over current protection that will also shut down the output voltage if the operating current of the pump is abnormally high or in the event of a short circuit.

The scroll pump operates on 120 VAC, single phase, 60 Hz and will be controlled by a Nationally Recognized Testing Laboratory (NRTL) approved motor control circuit with thermal overload protection.

The vacuum valves will be electropneumatic and require compressed air up to 125 psi. The 125 psi compressed air system will comply with Chapter 32 of the LLNL "Health and Safety Manual", "Pressure Safety", which is in accordance with all applicable ASME and DOT codes and regulations. Failure in the compressed air lines are usually the result of a damaged hose or improperly installed pneumatic fitting. Hoses and fittings of the proper rating should be inspected after installation and also periodically afterwards. The solenoids on the electropneumatic valves will be 24 VDC, which is classified as low voltage.

The vacuum valves will be normally closed valves, so that in the event of a power failure, the valves will close and isolate the vacuum if the compressed air system has an adequate reservoir.

7 Procurement / Fabrication Plan

7.1 Hardware Costs/Procurement Plan/QA Plan

All components recommended in this preliminary design are standard catalog items that do not require any development. Cost estimates were made for purchasing all hardware required for the complete vacuum system. Also not included are the spare parts. Suggested vendors are for reference only. Similar components by other manufacturers will be considered in the final design. The summary is listed in Table 7.1.Estimated procurement costs (Bill of Materials) for the ATTENUATOR vacuum system is listed in Table 7.2, 7.3 and 7.4.

In the Final Design phase, procurement documents including the detailed performance specification for all components will be prepared. These items will be sent out for bid to DOE/LLNL specified vendors and purchased by the LLNL procurement department. They will be subject to Final/Approved Detail Drawings and LLNL Mechanical Engineering Department Specifications. Established LLNL ISM and Quality Assurance Procedures will be followed. All selected materials will meet ASTM specifications and/or LLNL approval.

7.2 Fabrication and Testing Plan

Fabrication, preliminary assembly and testing of the vacuum pumping components are planned to take place at the LLNL Vacuum Sciences and Engineering Lab (Fig. 7.1 and 7.2). The facility provides ample room for complete module system assembly and testing. There is a wide variety of hardware and software in the LLNL Vacuum Sciences and Engineering Lab that will be available for recording experimental data. All technical staff will receive required vacuum technical training as specified by all LLNL LCLS IWS's.

Fabrication of all vacuum components must comply with the specifications listed below.

1. MEL95-001818-00, "Fabrication and Handling of Components for Ultra-High Vacuum Environment", Mechanical Engineering Department, LLNL, University of California.
2. ENC-93-910-REV 01, "Cleaning Stainless Steel Alloy Components", Mechanical Engineering Department, LLNL, University of California.
3. ENC-93-912-REV 01, "Cleaning Copper and Copper Alloy Components", Mechanical Engineering Department, LLNL, University of California.
4. MEL95-001817-00, "Welding of Stainless Steel components of Ultra-High Vacuum Environment", Mechanical Engineering Department, LLNL, University of California.

Preserving the cleanliness of the components during installation is essential in order to meet the required pressures in a timely manner. It is recommended that the LCLS facility develop a written installation procedure for all vacuum systems for training technical staff.

7.3 Prototype Plan

The final design of the attenuator system will be prepared based on the operation of a prototype beam sections at LLNL. One subassembly that contains pumping sections and structures (Fig. 7.3.1) will be fabricated and tested. The PLC and EPICS control software will also be developed and simulated. When completed, the assembly and parts will be shipped from LLNL to SLAC. Most of the parts of the system such as the pump crosses, foreline valves and stand components may be used in the actual attenuator system.

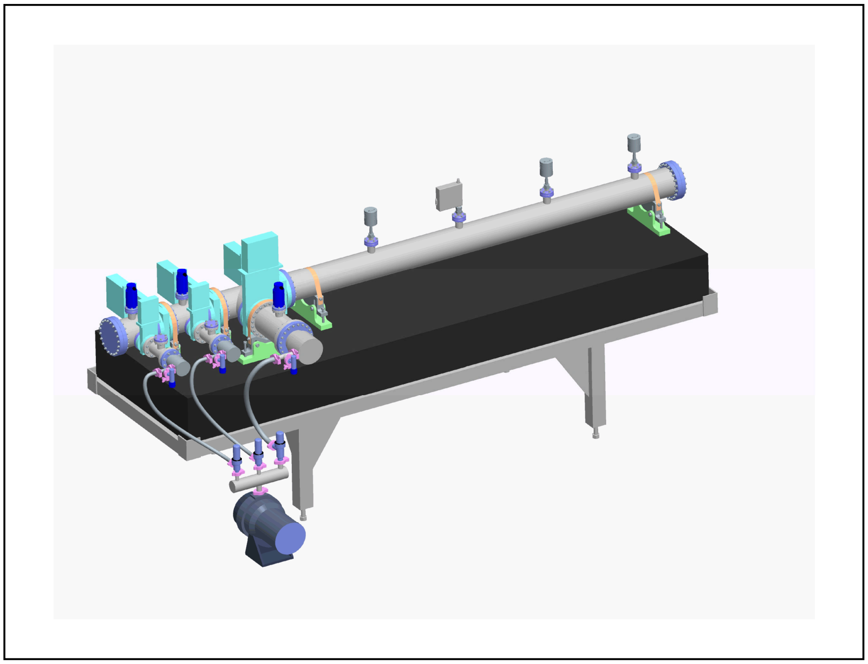

Fig. 7.3.1: Conceptual Layout of Gas Attenuator Prototype

8 System Design and Project Schedule

The overall schedule for completing the preliminary and final design, procurement, assembly, testing, and the installation of the attenuator vacuum system is presented in Fig. 8.1 and 8.2. Current schedule meets the following major project milestone:

1. Conceptual Design Review (4/06)
2. Prototype Testing (5/06)
3. Engineering Specification Document (6/06)
4. Preliminary Design Review (12/06)
5. Final Design Review (2/07)
6. Complete Procurement (6/07)
7. Sub assembly and Testing (8/07)
8. FEE Beneficial Occupancy (8/07)

9 Summary

The system concept design of the attenuator is completed. The major subjects presented in this report are:

1. Design of the complete attenuator system.
2. System analysis results.
3. ES&H issues and plan.
4. Project cost estimates and schedule.

All deliverables planned in the system concept design phase for attenuator system is presented herein. It is shown that the designed system:

1. Is consistent with the interface requirements of the attenuator system.
2. Is a robust and redundant system capable of providing the required vacuum level for attenuator operation with comfortable margin.
3. Is compliant with ES&H requirements.
4. Can be procured and fabricated with standard catalog items at reasonable costs, and meeting the LCLS schedule.

<u>We are ready to proceed with the Preliminary Design phase of the project</u>.

References

1. LCLS-PRD-1.5-003 “Physics Requirements for the XTOD Attenuator System”, 3/15/2006
2. Web site: http://physics.nist.gov/PhysRefData/FFast/html/form.html
3. J.M. Lafferty, “ Foundations of Vacuum Science and technology”, John Wiley & Sons, Inc.
4. LCLS-TN-06-1 **"The Physics Analysis of a Gas Attenuator with Argon as a Working Gas."** UCRL-TR-217980 (January 2006) D.D. Ryutov, R.M. Bionta, M.A. McKernan, S. Shen, J.W. Trent**,**